

ABSORPTION OF 10 GeV–1 TeV GAMMA RAYS BY RADIATION FROM BROAD-LINE REGION IN 3C 279

H. T. Liu¹, J. M. Bai¹, and L. Ma²

ABSTRACT

In this paper, we study the photon-photon pair production optical depth for 10 GeV–1 TeV gamma rays from 3C 279 due to the diffuse radiation of broad-line region (BLR). Assuming a power-law spectrum of $E_\gamma^{-a_2}$ for the photon intensity of very high energy (VHE) gamma rays, $a_1 \gtrsim 405$ and $a_2 \gtrsim 6.4$ are inferred by the integrated photon fluxes measured by MAGIC and HESS. Based on this power-law spectrum, the pre-absorbed spectra are inferred by correcting the photon-photon absorption on the diffuse photons of the BLR (internal absorption) and the extragalactic background light (external absorption). Position of gamma-ray emitting region R_γ determines the relative contributions of this two diffuse radiation to the total absorption for 10 GeV–1 TeV gamma rays. The internal absorption could make spectral shape of gamma rays more complex than only corrected for the external absorption, and could lead to the formation of arbitrary softening and hardening gamma-ray spectra. It should be necessary for the internal absorption to be considered in studying 10 GeV–1 TeV gamma rays from powerful blazars. The energies of annihilated gamma-ray photons due to the internal absorption are likely to be mainly reradiated around GeV. Our results indicate that R_γ may be between the inner and outer radii of the BLR for 3C 279. This implies for powerful blazars that R_γ might be neither inside the BLR cavity nor outside the BLR, but be within the BLR shell. Observations of *GLAST*, MAGIC, HESS, and VERITAS in the near future could give more constraints on the position of the gamma-ray emitting region relative to the BLR.

Subject headings: gamma rays: theory — quasars: individual (3C 279)

¹National Astronomical Observatories/Yunnan Astronomical Observatory, Chinese Academy of Sciences, Kunming, Yunnan 650011, China; liuhongtao1111@hotmail.com; baijinming@ynao.ac.cn

²Physics Department, Yunnan Normal University, Kunming 650092, China; send offprint requests to liuhongtao1111@hotmail.com

1. INTRODUCTION

The classical flat spectrum radio quasar (FSRQ) 3C 279 is one of the brightest extragalactic objects in the gamma-ray sky. It was detected by the EGRET, and its spectrum does not show any signature of gamma-ray absorption by pair production up to ~ 10 GeV (Fichtel et al. 1994; von Montigny et al. 1995). With the detection of high energy gamma rays in 66 blazars, containing 51 FSRQs and 15 BL Lac objects, in the GeV energy range by the EGRET experiment aboard the Compton Gamma Ray Observatory (Catanese et al. 1997; Fichtel et al. 1994; Lin et al. 1997; Mukherjee et al. 1997; Thompson et al. 1995, 1996; Villata et al. 1997; Hartman et al. 1999; Nolan et al. 2003), an exceptional opportunity is presented for the understanding of the central engine operating in blazars. Some of blazars have been also firmly detected by atmospheric Cerenkov telescopes at energies above 1 TeV, such as Mrk 421 (Punch et al. 1992), and Mrk 501 (Quinn et al. 1996). The High Energy Stereoscopic System (HESS) is an imaging atmospheric Cerenkov detector with the energy threshold above 100 GeV (Funk et al. 2004; Hinton 2004; Hofmann 2003). The Very Energetic Radiation Imaging Telescope Array System (VERITAS) provides unprecedented sensitivity to photon energies between 50 GeV and 50 TeV (see e.g., Holder et al. 2006). The Major Atmospheric Gamma Imaging Cerenkov telescope (MAGIC) is currently the largest single-dish Imaging Air Cerenkov Telescope in operation with the lowest energy threshold, ~ 30 GeV, among the new Cerenkov telescopes (see e.g., Baixeras et al. 2004). At present, 23 active galactic nuclei (AGNs) have been detected in very high energy (VHE) gamma rays, containing 21 BL Lac objects, one radio source M87, and the first FSRQ 3C 279 with the highest redshift $z = 0.536$ in these VHE AGNs¹. The MAGIC telescope detected VHE gamma rays from 3C 279 (Teshima et al. 2007). HESS observations measured an upper limit of integrated photon flux (Aharonian et al. 2008). The Large Area Telescope instrument on the Gamma-Ray Large Area Space Telescope (*GLAST*), the new-generation high energy gamma-ray telescope with sufficient angular resolution to allow identification of a large fraction of their optical counterparts, will observe gamma rays with energies from 20 MeV to greater than 300 GeV, and have the unique capability to detect thousands of gamma-ray blazars to redshifts of at least $z = 4$ (see e.g., Chen et al. 2004). *GLAST* was launched on June 11 2008. *GLAST*, combined with new-generation TeV instruments such as MAGIC, HESS, and VERITAS, will tremendously improve blazar spectra studies, filling in the band from 20 MeV to 10 TeV with high significance data for hundreds of AGNs (see Gehrels & Michelson 1999). Future measurements of the gamma-ray spectrum shape and its variability of blazars would tremendously improve our understanding to blazars.

¹<http://www.mppmu.mpg.de/~rwagner/sources/>

These gamma rays from blazars are generally believed to be attributed by emission from a relativistic jet oriented at a small angle to the line of sight (Blandford & Rees 1978). These gamma-ray components are contributed by inverse Compton emissions, including synchrotron self-Compton (SSC) scattering synchrotron seed photons, and external Compton (EC) scattering seed photons from sources outside the jet (see e.g., Böttcher 1999). The diffuse radiation fields of broad-line region (BLR) could have a strong impact on the expected EC spectra of powerful blazars, FSRQs (Liu & Bai 2006; Reimer 2007; Tavecchio & Ghisellini 2008). The external soft photon fields not only provide target photons for the EC processes to produce these gamma-ray components, but also absorb gamma rays from the EC processes, because gamma rays between 10 GeV and 1 TeV interact with infrared-ultraviolet photons to be attenuated by photon-photon pair production. Many efforts to study the absorption of gamma rays focus on the photon-photon annihilation by the diffuse extragalactic background radiation at the infrared (IR), optical, and ultraviolet (UV) bands (see e.g., Stecker et al. 1992, 2006, 2007; Stecker & de Jager 1998; Oh 2001; Renault et al. 2001; Chen et al. 2004; Dwek & Krennrich 2005; Schroedter 2005). This external absorption of gamma rays on the diffuse extragalactic background light (EBL) is also proposed and used to probe the EBL (Renault et al. 2001; Chen et al. 2004; Dwek & Krennrich 2005; Schroedter 2005). Indeed, the internal absorption of gamma rays inside FSRQs could result in serious problem for the possibility to use the external absorption of gamma rays to probe the IR–optical–UV extragalactic background, because the intrinsic spectra of gamma rays are masked by the internal absorption inside blazars (Donea & Protheroe 2003; Liu & Bai 2006; Reimer 2007). The intrinsic spectra of gamma rays are complicated by the complex spectra of the diffuse radiation fields of the BLRs in FSRQs (Tavecchio & Ghisellini 2008). The mean of intrinsic spectral index is around 2.3 for 17 BL Lac objects detected in the VHE regime (Wagner 2008).

The positions of gamma-ray emitting regions are still an open and controversial issue in the researches on blazars. It is suggested that gamma rays are produced inside the BLRs and the gamma-ray emitting radius R_γ ranges roughly between 0.03 and 0.3 pc (Ghisellini & Madau 1996). It is argued by Georganopoulos et al. (2001) that the radiative plasma in relativistic jets of powerful blazars are within cavities formed by the BLRs. However, other researchers argued that the gamma-ray emitting regions are outside the BLRs (Lindfors et al. 2005; Sokolov & Marscher 2005). In our previous research (Liu & Bai 2006, hereafter Paper I), the position of gamma-ray emitting region is a key parameter to determine whether high energy gamma rays could escape the diffuse radiation fields of the BLRs for FSRQs. It is unknown whether these gamma rays could be detected by *GLAST*, *MAGIC*, *HESS*, and *VERITAS* even if blazars intrinsically produce 10 GeV–1 TeV gamma rays, because the gamma-ray emitting radii are unknown. These gamma rays around 200 GeV is optically

thick for 3C 279 if the emitting region is within the BLR cavity (see Paper I). However, the MAGIC observations on 2006 February 23 have shown a clear gamma-ray signal in the VHE regime (Teshima et al. 2007). This indicates that the emitting region of these VHE gamma rays should not be inside the BLR cavity, otherwise, the intrinsic flux of these VHE gamma rays is likely to be extremely high. In Paper I, we addressed an important topic in gamma-ray astrophysics, namely the absorption of high energy gamma rays inside of FSRQs by photons of the BLR. In this paper, we attempt to address the particular topic of absorption in the gamma-ray quasar 3C 279 using the available observational data, and its potential effect on the spectra of gamma rays. In order to constrain the position of gamma-ray emitting region in 3C 279, we study the internal absorption of gamma rays by the diffuse radiation from the BLR and its potential effect on the spectra of gamma rays from 10 GeV to 1 TeV.

The structure of this paper is as follows. § 2 presents intensity of VHE gamma rays. § 3 presents theoretical calculation, and consists of two subsections. § 3.1 presents calculations of temperature profiles, and § 3.2 photon-photon optical depth for 3C 279. § 4 presents external absorption on IR–optical–UV extragalactic background. § 5 is spectral shape of VHE gamma rays. § 6 presents pair spectrum due to photon-photon annihilation and their radiation. § 7 is for discussions and conclusions. Throughout this paper, we use a flat cosmology with a deceleration factor $q_0 = 0.5$ and a Hubble constant $H_0 = 75 \text{ km s}^{-1} \text{ Mpc}^{-1}$.

2. INTENSITY OF VHE GAMMA RAYS

The classical FSRQ 3C 279 is one of the brightest extragalactic objects in the gamma-ray sky, and it is also the first VHE gamma-ray FSRQ. For 3C 279, there are ten MAGIC observation nights from 2006 January 31 to 2006 March 31. While in most of the nights gamma-ray fluxes compatible with zero were observed, a marginal signal was seen during the 2006 February 22 observations. In the night of 2006 February 23, observations have shown a clear gamma-ray signal with an integrated photon flux $F(E_\gamma > 200 \text{ GeV}) = (3.5 \pm 0.8) \times 10^{-11} \text{ cm}^{-2}\text{s}^{-1}$ (Teshima et al. 2007). This gamma-ray detection was not accompanied by an optical flare or by particularly high flux levels or outbursts in X-rays (Teshima et al. 2007). After one day, 3C 279 brightens from a marginal signal to a clear signal detected by MAGIC. This suggests that the VHE gamma-ray emissions may have variations on the order of days. The GeV gamma-ray emissions detected by the EGRET have variations on timescale as short as 1 day (Hartman et al. 2001a). This variation timescale is roughly consistent with that observed by MAGIC. This agreement indicates that the GeV and VHE gamma rays may have some certain relationship. However, no VHE spectrum of 3C 279 has been published yet.

For 3C 279, observations on 2006 February 22–23 show the optical R magnitude around 14.5 (see Fig. 1 in Böttcher et al. 2007), and a flux density around 5–5.2 mJy in the R band (see Fig. 1 in Teshima et al. 2007). The average of R band magnitude on 2000 February 8 to March 1 is around 14.5 (see Fig. 2 in Kartaltepe & Balonek 2007). The simultaneous multi-wavelength observations on 2000 February 8 to March 1 for 3C 279 show a flux density from 4.2 to 8.9 mJy in the R band (Hartman et al. 2001b). These R band magnitudes and flux densities observed on 2000 February 8 to March 1 are consistent with those observed on 2006 February 22–23. This agreement indicates that the gamma-ray emissions on this two periods are likely to have very similar states. Thus, the gamma-ray emissions on 2006 February 22–23 are likely to be at mediate states. The gamma-ray emissions in most of the nights when gamma-ray fluxes compatible with zero were observed are likely to be at low states.

Though, an integrated photon flux is given by Teshima et al. (2007), no VHE spectrum of 3C 279 has been published. Fortunately, HESS observations in 2007 January measured an upper limit of integrated photon flux $F(E_\gamma > 300 \text{ GeV}) < 3.98 \times 10^{-12} \text{ cm}^{-2}\text{s}^{-1}$ (Aharonian et al. 2008). Observations show that VHE spectra of these known VHE sources can be described by a power-law spectrum (see Wagner 2008). Thus, a power-law spectrum of $\frac{dI}{dE_\gamma} = a_1 E_\gamma^{-a_2}$ is assumed for the photon intensity of the VHE gamma rays. This VHE gamma-ray spectrum could be limited by the two measured integrated photon fluxes. Taking into account the integrated photon fluxes measured by MAGIC and HESS: adopting $F(E_\gamma > 200 \text{ GeV}) = 3.5 \times 10^{-11} \text{ cm}^{-2}\text{s}^{-1}$ and assuming $F(E_\gamma > 300 \text{ GeV}) = 3.9 \times 10^{-12} \text{ cm}^{-2}\text{s}^{-1}$, the photon intensity of the VHE gamma rays is inferred as

$$\frac{dI}{dE_\gamma} = 505 \times E_\gamma^{-6.4} \text{ cm}^{-2}\text{s}^{-1}\text{GeV}^{-1}. \quad (1)$$

Though, $a_2 \gtrsim 6.4$ is limited by the HESS observations, we will adopt $a_2 = 6.4$ in the following calculations, and will discuss the potential effect of $a_2 \gtrsim 6.4$ on our results in the last section. The spectral slope of 6.4 is larger than that of any other known VHE sources (see Wagner 2008). The maximum spectral slope of 4.21 has been measured in the VHE regime for PG 1553+113 (Albert et al. 2007). This spectral slope of 6.4 is also larger than the slope of 2.3 for the extrapolated VHE spectrum by the GeV spectrum observed on 2000 February 8 to March 1 (Hartman et al. 2001b). The average EGRET blazar spectrum was found to have a slope of 2.27 (Venters & Pavlidou 2007). The mean of intrinsic spectral indices is $\bar{\Gamma} \approx 2.3$ for 17 blazars detected in the VHE regime (see Wagner 2008). The reason that this spectral slope of 6.4 is larger than any other known photon index of gamma rays, measured and intrinsic spectral indices, is likely to be the internal and external absorption of gamma rays by the diffuse radiation fields of the BLR and the EBL. Stecker et al. (1992) investigated the photon-photon absorption of the VHE gamma-ray spectrum, extrapolated

by the differential spectrum of gamma rays measured by EGRET during 1991 June, on the extragalactic background infrared radiation field. The corrected photon flux is not inconsistent with the Whipple upper limit (Stecker et al. 1992). This indicates that the VHE and GeV gamma rays are likely to have some relationship. In the following section, we shall firstly calculate the internal absorption within 3C 279 by the diffuse radiation fields produced by the BLR.

3. THEORETICAL CALCULATION

As described in § 2.1, 2.2, and 2.3 of Paper I, equations (1)–(21) can be used to estimate the absorption optical depth by the diffuse radiation of the BLR, adopting the spherical shell of clouds (see Fig. 1 in Paper I) and the relative intensity of broad emission lines presented on Figure 2 in Paper I, and assuming a blackbody temperature in the inner regions of accretion disk. The assumption of the single-temperature blackbody probably differs significantly from the real cases. The surface effective temperatures of accretion disks are functions of radii r_d , i.e., $T_{\text{eff}} = T_{\text{eff}}(r_d)$ (see e.g., Ebisawa et al. 1991; Hanawa 1989; Li et al. 2005; Pereyra et al. 2006; Shakura & Sunyaev 1973; Zimmerman et al. 2005). These continua from thin accretion disks can be well described by multi-temperature blackbody. Considering the temperature profile of accretion disk, the factor $n_{\text{bb}}(\nu, T)$ in equations (20) and (21) in Paper I should be replaced by

$$n_{\text{bb}}(\nu, T) = \int_{X_{\text{in}}}^{X_{\text{out}}} n_{\text{bb}}(\nu, T_{\text{eff}}(X_d)) dX_d, \quad (2)$$

where $X_{\text{in}} = r_{\text{in}}/r_g$ and $X_{\text{out}} = r_{\text{out}}/r_g$ are the inner and outer radii of accretion disk, respectively, and $X_d = r_d/r_g$. The gravitational radius of a black hole with mass of M_{BH} is $r_g = GM_{\text{BH}}/c^2$, where G is the gravitational constant and c is the speed of light.

In the calculations of the photon-photon attenuation optical depth, the soft photon frequency is considered in the range from $\nu_2^L = 10^{12.0}$ Hz to $\nu_2^U = 10^{16.5}$ Hz for the diffuse continuum from the BLR. The temperature profile of accretion disk is considered for standard thin accretion disk.

3.1. Calculations of Temperature Profiles

The local effective temperatures of accretion disks are functions of radii r_d (see e.g., Ebisawa et al. 1991; Hanawa 1989; Li et al. 2005; Pereyra et al. 2006; Shakura & Sunyaev 1973; Zimmerman et al. 2005). The standard accretion disk is the basic model for a

radiatively efficient, geometrically thin disk. Variability of active galactic nuclei is mostly in favor of the standard accretion disk models of AGNs (Liu et al. 2008). Although, equations required to calculate the temperature profile are the same as equations (5)–(12) in our previous paper (Liu et al. 2008), they are presented as equations (A1)–(A8) to make this paper more readable (see Appendix A). For high luminosity blazars showing a clear UV bump, the ironing luminosity $L_{\text{iron}} = L_{\text{UV}} = \eta \dot{M} c^2$ according to the definition of the efficiency η with which various types of black holes convert rest mass-energy into outgoing radiation (Thorne 1974). From the observed BLR luminosity L_{BLR} and relation $L_{\text{BLR}} = f_{\text{cov}} L_{\text{UV}}$ (D’Elia et al. 2003), we could estimate the mass accretion rate of the central black hole by the formula

$$\dot{M} = \frac{L_{\text{UV}}}{\eta_{\text{max}} c^2} = \frac{L_{\text{BLR}}}{\eta_{\text{max}} f_{\text{cov}} c^2}. \quad (3)$$

The temperature profiles could be estimated by equations (A1)–(A8) and equation (3).

The dimensionless spin parameter of a black hole can take on any value in the range $-1 \leq a_* \leq 1$, where negative values of a_* correspond to a black hole that retrogrades relative to its accretion disk. For simplicity we consider only prograde spins up to the Thorne spin equilibrium limit, i.e. $0 \leq a_* \leq 0.998$ (Thorne 1974). Recent work on magnetohydrodynamic accretion disks suggest a rather lower equilibrium spin (see e.g., Gammie et al. 2004; Krolik et al. 2005). Spin equilibrium is reached at $a_* \approx 0.93$ through accretion of gases onto the central black hole, and mergers of black holes with comparable mass can result in a final spin of $a_* \sim 0.8$ – 0.9 (Gammie et al. 2004). Equilibrium spins as low as $a_* \sim 0.9$ are within the realm of possibility (Krolik et al. 2005). Aschenbach et al. (2004) obtained a value of $a_* = 0.9939^{+0.0026}_{-0.0074}$ for the Galactic Center black hole. Brenneman & Reynolds (2006) obtained a formal constraint on spin $a_* = 0.989^{+0.009}_{-0.002}$ at 90% confidence for the Seyfert galaxy MCG–06-30-15. Considering the probable ranges of spin parameter a_* suggested above, we take three values of spin parameter $a_* = 0.5, 0.8, \text{ and } 0.998$ in the Kerr metric to calculate the temperature profiles. Combining equations (A1)–(A8), equation (3), and the parameters of $M_{\text{BH}}, L_{\text{BLR}}, f_{\text{cov}}, \text{ and } a_*$, the surface effective temperature profiles are calculated. The calculated results are presented in Figure 1.

3.2. Photon-Photon Optical Depth For 3C 279

As stated in §5 of Paper I, the absorption of gamma rays by emission lines is unrelated to the BLR covering factor f_{cov} , and the gamma-ray absorption by the diffuse blackbody radiation is in proportion to the ratio $\tau_{\text{BLR}}/f_{\text{cov}}$, where τ_{BLR} is the Thomson optical depth of BLR. Various values of the BLR covering factor are suggested and estimated. Early estimates of this quantity indicated a covering factor $f_{\text{cov}} \sim 5$ – 10% , while recent observations indicated

$f_{\text{cov}} \sim 30\%$ (see e.g., Maiolino et al. 2001). D’Elia et al. (2003) found only two blazars in literatures: 3C 273 and PKS 2149-306, of which both UV continuum emission from accretion disks and broad emission lines have been measured. They obtained $f_{\text{cov}} \sim 7\%$ for the first source and $f_{\text{cov}} \sim 10\%$ for the second one. Donea & Protheroe (2003) suggested $f_{\text{cov}} \sim 3\%$ for the spherical distribution of the BLR clouds in quasars. The issue of the Thomson optical depth of BLR has rarely been studied and has gotten nowhere for blazars. Blandford & Levison (1995) adopted the Thomson optical depth of BLR as $\tau_{\text{BLR}} = 0.01$. Thus, the ratio of $\tau_{\text{BLR}}/f_{\text{cov}}$ is likely to be typically of order $\tau_{\text{BLR}}/f_{\text{cov}} \sim 1$ for the spherical distribution of the BLR clouds in blazars. In the calculations of $\tau_{\gamma\gamma}$, we adopted $\tau_{\text{BLR}}/f_{\text{cov}} = 1$ and $f_{\text{cov}} = 0.03$ for the spherical distribution of the BLR clouds in FSRQs.

3C 279 has a BLR luminosity $L_{\text{BLR}} = 10^{44.41}$ ergs s^{-1} (Cao & Jiang 1999), and a black hole mass of $M_{\text{BH}} = 10^{8.4} M_{\odot}$ (Woo & Urry 2002). It was detected by the EGRET in the 0.1–10 GeV energy domain, and its spectrum can be fitted by a power law without any signature of gamma-ray absorption by pair production (Fichtel et al. 1994; von Montigny et al. 1995). Firstly, we investigated the dependence of the effective temperature T_{eff} on the central black hole spin a_* for 3C 279. The inner radii of accretion disks in the Kerr potential are fixed at the marginally stable orbit $r_{\text{ms}}(a_*) = X_{\text{ms}}(a_*)r_{\text{g}}$. The outer radii of accretion disks are fixed at $r_{\text{out}} = 200r_{\text{g}}$. The temperature profiles of the standard accretion disks are presented in Figure 1. It is obvious that the temperatures for three different values of a_* are nearly the same at the radius $r_{\text{out}} = 200r_{\text{g}}$. The variations of a_* can significantly change the temperature profiles (see Fig. 1). It is evident that the different temperature profiles produce different multi-temperature blackbody continua, and then could result in different absorption for gamma rays.

We calculated $\tau_{\gamma\gamma}$ for 3C 279 by adopting the BLR inner radius $r_{\text{BLR,in}} = 0.1$ pc and the BLR outer radius $r_{\text{BLR,out}} = 0.4$ pc from Hartman et al. (2001b). It is suggested that the gamma-ray emitting region should be within the BLR cavity (Ghisellini & Madau 1996; Georganopoulos et al. 2001). Firstly, we assume $R_{\gamma} = r_{\text{BLR,in}}$ to calculate the absorption optical depth. The absorption optical depth is presented in Figure 2. It can be seen in Figure 2 that the diffuse radiation fields of the BLR are not transparent to gamma rays of energies from 10 GeV to 1 TeV in the observer frame if these gamma rays are inside the BLR cavity. This result is inconsistent with observations that show no signature of gamma-ray absorption by pair production around 10 GeV (see e.g., Fichtel et al. 1994; von Montigny et al. 1995; Ghisellini & Madau 1996; Wehrle et al. 1998). Thus for ~ 10 GeV gamma rays, observations should not support suggestions of gamma-ray emitting region within the BLR cavity. It is likely that the gamma-ray emitting region is within the BLR, i.e. $r_{\text{BLR,in}} < R_{\gamma} < r_{\text{BLR,out}}$. The absorption optical depth is calculated by assuming $R_{\gamma} = (r_{\text{BLR,out}} + r_{\text{BLR,in}})/2$ (see Fig. 3). It is obvious that the VHE gamma rays are still significantly absorbed by the diffuse

radiation of the BLR (only $\sim 5\%$ escape probability). These 10 GeV gamma rays are still slightly absorbed. The slightly larger cover factor f_{cov} could make it vanish for this slight absorption around 10 GeV. Thus, the gamma-ray emitting region is likely to be within the BLR. The gamma-ray emitting regions outside the BLRs are argued by some researchers (Lindfors et al. 2005; Sokolov & Marscher 2005). Therefore, $R_\gamma = r_{\text{BLR,out}}$ is assumed to calculate the absorption optical depth. The calculated results are presented in Figure 4. There is no absorption for 10 GeV gamma rays (see Fig. 4). This is consistent with the EGRET observations. For the VHE gamma rays, greater than $\sim 60\%$ of the primary gamma rays can escape the diffuse radiation fields of the BLR (see Fig. 4).

4. EXTERNAL ABSORPTION ON IR-OPTICAL-UV EXTRAGALACTIC BACKGROUND

Many efforts are focused on investigating the EBL at IR–optical–UV bands, and the photon-photon annihilation absorption of gamma rays by the EBL at these bands (see e.g., Stecker et al. 1992; Stecker & de Jager 1998; Oh 2001; Renault et al. 2001; Chen et al. 2004; Dwek & Krennrich 2005; Schroedter 2005). The external absorption of gamma rays by the diffuse EBL is also proposed and used to probe the EBL (Renault et al. 2001; Chen et al. 2004; Dwek & Krennrich 2005; Schroedter 2005). Stecker et al. (1992) first pointed out the importance of the EBL in determining the opacity of the universe to high energy gamma rays at higher redshifts. Dwek & Krennrich (2005) detailed the observational limits and detections of the EBL, and the relevant EBL spectral templates. Their investigations showed that the absorption of gamma rays $\lesssim 1$ TeV is entirely contributed by the EBL at 0.1–10 μm (see Fig. 3 in Dwek & Krennrich 2005). Dwek & Krennrich only calculated the optical depth for low redshift sources. Stecker et al. (2006, 2007) have given the optical depth for sources at redshifts < 6 . Stecker et al. (1992) investigated the IR EBL absorption on high energy gamma rays for 3C 279, and got absorption optical depth of $3.7 \lesssim \tau \lesssim 9.7$ for 1 TeV gamma rays. An analytic form to approximate the function $\tau_{\gamma\gamma}(E_\gamma, z)$ of the external EBL absorption is given as (Stecker et al. 2006)

$$\log \tau_{\gamma\gamma} = Ax^4 + Bx^3 + Cx^2 + Dx + E, \quad (4)$$

where $x \equiv \log E_\gamma(\text{eV})$. Coefficients A through E are given in Table 1 for various redshifts (Stecker et al. 2006, 2007). The parametric approximation holds for $10^{-2} \leq \tau_{\gamma\gamma} \leq 10^2$ and $E_\gamma \lesssim 2$ TeV. These coefficients at redshift $z = 0.5$ for the baseline model fit are adopted to calculate the EBL absorption optical depth.

In order to compare the internal and external absorption, the calculated results for the external absorption are also presented in Figures 2a, 3a, and 4a. If R_γ is around the inner

radius $r_{\text{BLR,in}}$, the internal absorption dominates over the external absorption, and the latter mainly presents itself in the VHE interval and is much less than unity around 10 to a few ten GeV (see Fig. 2a). The internal absorption peaks around 200 GeV, and the external absorption increases with energies of gamma rays (see Fig. 2a). If R_γ is around the median of $r_{\text{BLR,in}}$ and $r_{\text{BLR,out}}$, the total absorption is dominated by the internal absorption in the interval of 10–100 GeV, and the external absorption dominates over the internal one from 300 GeV to 1 TeV (see Fig. 3a). The relative contributions of the internal and external absorption to the total one are comparable around 200 GeV (see Fig. 3a). If R_γ is around the outer radius $r_{\text{BLR,out}}$, the internal absorption is comparable with the external one from 10 to 20 GeV, and the former is dominated by the latter in the interval of 30 GeV to 1 TeV (see Fig. 4a). The positions of gamma-ray emitting regions determine the relative contributions of the internal and external absorption to the total photon-photon annihilation optical depth for 10 GeV–1 TeV gamma rays.

5. SPECTRAL SHAPE OF VHE GAMMA RAYS

Measured and intrinsic VHE gamma-ray spectra can be well described by a power-law spectrum, and intrinsic gamma-ray spectra of 17 BL Lac objects are inferred by only correcting the EBL absorption to the measured spectra (e.g., Wagner 2008). If the gamma-ray emitting regions are far from the BLRs in FSRQs, it is reasonable to infer the intrinsic spectra by only correcting the EBL absorption. Otherwise, it is likely to be insufficient for FSRQs to infer the intrinsic spectra from the measured VHE spectra by only correcting the EBL absorption, because the internal absorption is not negligible when compared with the external absorption (see Figs. 2a and 3a). The positions of gamma-ray emitting regions determine the relative contributions of the internal and external absorption. The dependence of the internal absorption on energies of gamma rays relies on the positions of gamma-ray emitting regions (see Figs. 2a, 3a, and 4a). The external absorption monotonically increases with energies of gamma rays, and then its effect on the spectral shape is more straightforward than that of the internal absorption. It is obvious that the external absorption softens the observed gamma-ray spectrum relative to the emission one.

In order to study the dependence of the internal absorption on the gamma-ray emitting radius R_γ , we accepted gamma-ray energy $E_\gamma = 50, 100, 300, 500, \text{ and } 1000$ GeV to calculate the photon-photon absorption optical depth. The calculated results are presented in Figure 5. It is obvious that the absorption optical depth $\tau_{\gamma\gamma}$ rapidly decreases with increasing R_γ , because the energy density of the diffuse radiation of the BLR rapidly decreases beyond $r_{\text{BLR,in}}$. For a fixed E_γ , $\tau_{\gamma\gamma}$ monotonically decreases as R_γ increases. For a fixed R_γ , the

dependence of $\tau_{\gamma\gamma}$ on E_γ relies on R_γ . The internal absorption optical depth $\tau_{\gamma\gamma}$ of VHE gamma rays does not monotonically vary with E_γ , and peaks around a few hundred GeV if $R_\gamma \lesssim 0.35$ pc (see Fig. 5). This is confirmed by these calculated results presented in Figures 2a and 3a. The optical depth $\tau_{\gamma\gamma}$ for any E_γ monotonically varies with E_γ if $R_\gamma \gtrsim 0.35$ pc (see Figs. 4a and 5). The optical depth $\tau_{\gamma\gamma}$ of high energy gamma rays monotonically increases with E_γ for any R_γ (see Figs. 2a, 3a, 4a, and 5).

After gamma-ray spectra are corrected for the internal and external absorption, the pre-absorbed spectra are given for three values of R_γ (see dash-dot-dotted curves in Figs. 2b, 3b, and 4b). If R_γ is around $r_{\text{BLR,in}}$, the pre-absorbed VHE gamma-ray spectra peak around 200 GeV (see Fig. 2b). The internal absorption hardens the VHE gamma-ray spectrum around 300 GeV–1 TeV, and softens the gamma-ray spectrum below 200 GeV (see Fig. 2b). If R_γ is around the median of inner and outer radii of the BLR, the internal absorption softens the gamma-ray spectrum below ~ 400 GeV, and hardens the VHE gamma-ray spectrum from ~ 400 GeV to 1 TeV (see Fig. 3b). If R_γ is beyond the outer radius of the BLR, the internal absorption softens the gamma-ray spectrum (see Fig. 4b), and has the same effect as the external absorption. The external absorption softens these gamma-ray spectra that escape from the diffuse radiation fields of the BLR. After passing through the internal and external diffuse radiation fields, these detected gamma-ray spectra are softer than those pre-absorbed ones below ~ 400 GeV, and are harder than those pre-absorbed ones from ~ 400 GeV to 1 TeV, when R_γ is around $R_{\text{BLR,in}}$ (see Fig. 2b). As R_γ is beyond the median of inner and outer radii of the BLR, these detected gamma-ray spectra are softer than those pre-absorbed ones (see Figs. 3b and 4b). If the intrinsic spectral indices have a typical value of 2.3 for VHE gamma-ray sources, the first VHE FSRQ 3C 279 may have an intrinsic spectral index around 2.3 in the VHE regime. These pre-absorbed VHE gamma rays from 200 GeV to 1 TeV can be well fitted by a power-law spectrum with a chance probability of $p < 10^{-20}$. As $R_\gamma = 0.1$ pc, photon indices of 5.7 ± 0.2 ($a_* = 0.5$) and 4.9 ± 0.2 ($a_* = 0.998$) are given by fit. These values are larger than the typical value of 2.3 for those known VHE sources, and are also larger than the intrinsic photon index $\simeq 3.6$ for PG 1553+113, the maximum among those known VHE spectra (Wagner 2008). Photon indices of 1.97 ± 0.009 ($a_* = 0.5$) and 1.94 ± 0.003 ($a_* = 0.998$) are given for $R_\gamma = 0.25$ pc. These two values are smaller than the typical value of 2.3 in the VHE regime, but are larger than the intrinsic photon index $\simeq 1.3$ for 1ES 1101-232, the minimum among those known VHE spectra (Wagner 2008). Photon indices of 1.7 ± 0.03 are given for $R_\gamma = 0.4$ pc. This value is smaller than the typical value of 2.3, but is larger than the minimum of 1.3. If a_2 is allowed to rise, these fit photon indices for the pre-absorbed VHE spectra could be increased. Thus, it is unlikely for 3C 279 that these gamma-ray emitting regions are inside the BLR cavity.

6. PAIR SPECTRUM DUE TO PHOTON-PHOTON ANNIHILATION AND THEIR RADIATION

In this section, our efforts are focused on studying where energies of annihilated gamma-ray photons are likely to be reradiated. Böttcher & Schlickeiser (1997) derived the exact analytic solution of pair production spectrum from photon-photon annihilation, and showed that this exact solution is in very good agreement with the approximation of Aharonian et al. (1983), the most accurate one of the various approximations known before. The interaction of power-law gamma-ray spectra with thermal soft photon fields is generally described within an error of a few percent at all electron/positron energies if the soft photon temperature is $kT/m_e c^2 \lesssim 0.1$, even if gamma-ray spectra extend down to $\varepsilon_1 \sim 1$. Thus, we adopted the approximation of Aharonian et al. (see eq. [32] of Böttcher & Schlickeiser 1997) to estimate the pair injection rate $\frac{dn(\gamma)}{dt}$ due to photon-photon absorption by the diffuse radiation fields of the BLR in 3C 279. A power-law spectrum is assumed as $\propto E_\gamma^{-2.3}$ for the pre-absorbed gamma-ray spectrum in order to calculate the pair injection rate. For simplicity in the calculations of $\frac{dn(\gamma)}{dt}$, we adopted radial independent soft photon densities with such a relative intensity that can produce the comparable quantity of $\int \frac{dn(\gamma)}{dt} d\gamma$, converted from the energies of annihilated gamma-ray photons, for the diffuse multi-temperature blackbody and broad emission lines. After the soft photon densities and the pair production rate $\frac{dn(\gamma)}{dt}$ are given, the equilibrium pair distribution of steady state could be estimated. Figure 6a shows the differential pair injection rate $\frac{dn(\gamma)}{dt}$ for the interaction of a power-law gamma-ray spectrum $\propto E_\gamma^{-2.3}$ with the BLR diffuse radiation of 3C 279. The γ values of electrons/positrons annihilated from the broad emission lines and gamma rays have a lower limit of $\gamma \gtrsim 10^4$ (see Fig. 6a). The γ values of electrons/positrons from annihilation between the multi-temperature blackbody and gamma rays have a lower limit of $\gamma \gtrsim 10^3$ (see Fig. 6a).

If considering the radiative cooling, synchrotron cooling and external Compton scattering cooling, the equilibrium pair distribution of steady state is $n(\gamma) = \int_\gamma^{\gamma_{\max}} \frac{dn(\gamma)}{dt} d\gamma / \dot{\gamma}$, where $\dot{\gamma} = \dot{\gamma}_{\text{syn}}(\gamma) + \dot{\gamma}_{\text{EC}}(\gamma)$, and $\gamma = E_{e^\pm}/m_e c^2$ is electron/positron energy. The synchrotron cooling rate is given by the formula $\dot{\gamma}_{\text{syn}}(\gamma) = \frac{4}{3} \frac{\sigma_{\text{Th}}}{m_e c} \frac{B^2}{8\pi} \gamma^2$, where B is the magnetic field intensity. The EC scattering cooling rate is $\dot{\gamma}_{\text{EC}}(\gamma) = \int d\varepsilon_1 \varepsilon_1 \int F_{\text{KN}}(\varepsilon_1, \varepsilon_2, \gamma) n(\varepsilon_2) d\varepsilon_2$, where we use the Compton kernel F_{KN} for an isotropic soft photons, considering the full Klein-Nishina cross section (Jones 1968; Blumenthal & Gould 1970). The Compton kernel is

$$F_{\text{KN}} = \frac{3}{4} \frac{c\sigma_{\text{Th}}}{\varepsilon_2 \gamma^2} \left[2q \ln q + 1 + q - 2q^2 + \frac{(\gamma_{\varepsilon_2} q)^2 (1 - q)}{2(1 + \gamma_{\varepsilon_2} q)} \right], \quad (5)$$

where $\gamma_{\varepsilon_2} = 4\varepsilon_2 \gamma$, $q = \frac{\varepsilon_1}{4\varepsilon_2 \gamma (\gamma - \varepsilon_1)}$, and $1/4\gamma^2 < q < 1$ (Jones 1968; Blumenthal & Gould 1970). ε_1 and ε_2 in this paper are energies of gamma rays and soft photons in units of $m_e c^2$,

respectively. The synchrotron emission coefficient is

$$j_{\text{syn}}(\nu) = \frac{\sqrt{3}e^3B}{4\pi m_e c^2} \int d\gamma n(\gamma) R_{\text{CS}}(x), \quad (6)$$

where the mean emission coefficient for a single electron/positron averaged over an isotropic distribution of pitch angles $R_{\text{CS}}(x)$ (Crusius & Schlickeiser 1986; Ghisellini et al. 1988) is

$$R_{\text{CS}}(x) = 2x^2 K_{4/3}(x) K_{1/3}(x) - \frac{6x^3}{5} [K_{4/3}^2(x) - K_{1/3}^2(x)], \quad (7)$$

where $x = \nu/3\gamma^2\nu_B$ and $\nu_B = eB/2\pi m_e c$, and K_n is the McDonald function of order n (see also Saugé & Henri 2004). The EC emission coefficient $j_{\text{EC}}(\nu)$ is

$$j_{\text{EC}}(\nu_1) = \frac{h}{4\pi} \varepsilon_1 \int \int F_{\text{KN}}(\varepsilon_1, \varepsilon_2, \gamma) n(\varepsilon_2) n(\gamma) d\gamma d\varepsilon_2, \quad (8)$$

where $n(\varepsilon_2)$ is the differential soft photon density. For 3C 279, we adopted the magnetic field intensity $B = 1.5$ G from Hartman et al. (2001b). The calculated spectra are presented in Figure 6b. For FSRQs, the ratio of the EC luminosity to synchrotron luminosity is $L_{\text{EC}}/L_{\text{syn}} \sim 10$, on average (Ghisellini et al. 1998; Georganopoulos et al. 2001). The relative radiation intensities of the diffuse blackbody and broad emission lines of the BLR and the magnetic field intensity, adopted in calculations, could produce the ratio of $L_{\text{EC}}/L_{\text{syn}} = \nu J_{\nu, \text{EC}}/\nu J_{\nu, \text{syn}} \sim 10$ for the pair spectrum due to photon-photon absorption (see Fig. 6b). It can be seen in Figure 6b that the synchrotron emissions peak around keV, and the EC emissions peak around GeV. Thus, the intense creation of pairs would produce a strong radiation at low energy X-rays and around GeV energy. These produced gamma rays around GeV, where the pileup of photons below the absorption threshold occurs, could result in a significant flattening in the observed spectrum relative to the emission spectrum.

7. DISCUSSIONS AND CONCLUSIONS

HESS observations in 2007 January measured an upper limit of integrated photon flux $F(E_\gamma > 300 \text{ GeV}) < 3.98 \times 10^{-12} \text{ cm}^{-2}\text{s}^{-1}$ (Aharonian et al. 2008). In calculations, we assumed $F(E_\gamma > 300 \text{ GeV}) = 3.9 \times 10^{-12} \text{ cm}^{-2}\text{s}^{-1}$, allowed by HESS observations. Combining this flux with integrated photon flux $F(E_\gamma > 200 \text{ GeV}) = 3.5 \times 10^{-11} \text{ cm}^{-2}\text{s}^{-1}$ measured by MAGIC (Teshima et al. 2007), a power-law spectrum of $\frac{dI}{dE_\gamma} = a_1 E_\gamma^{-a_2}$ is inferred with $a_1 = 505$ and $a_2 = 6.4$. If $F(E_\gamma > 300 \text{ GeV}) = 3.6 \times 10^{-12} \text{ cm}^{-2}\text{s}^{-1}$ is adopted for HESS observations, $a_1 = 1510$ and $a_2 = 6.6$. If $F(E_\gamma > 300 \text{ GeV}) = 3.98 \times 10^{-12} \text{ cm}^{-2}\text{s}^{-1}$ is adopted, $a_1 = 405$ and $a_2 = 6.36$. Thus $a_1 \gtrsim 405$ and $a_2 \gtrsim 6.4$ are likely to be limited by

MAGIC and HESS observations for a VHE gamma-ray spectrum of $\frac{dI}{dE_\gamma} = a_1 E_\gamma^{-a_2}$. Based on the gamma-ray spectrum of $\frac{dI}{dE_\gamma} = 505 E_\gamma^{-6.4}$ but corrected for the internal and external absorption (see Figs. 2b, 3b, and 4b), photon indices of these corrected VHE gamma rays are around 5 as $R_\gamma = 0.1$ pc, 2.0 as $R_\gamma = 0.25$ pc, and 1.7 as $R_\gamma = 0.4$ pc. These inferred photon indices as $R_\gamma = 0.25$ and 0.4 pc are inside of those known intrinsic photon indices. If $a_2 = 6.6$, photon indices of 1.9 ± 0.03 are inferred for $R_\gamma = 0.4$ pc, 2.2 ± 0.01 ($a_* = 0.5$) and 2.1 ± 0.003 ($a_* = 0.998$) for $R_\gamma = 0.25$ pc, and 6.0 ± 0.2 ($a_* = 0.5$) and 5.1 ± 0.2 ($a_* = 0.998$) for $R_\gamma = 0.1$ pc. As R_γ varies between 0.1 and 0.4 pc, photon indices of pre-absorbed VHE gamma-ray spectra are likely to be inside of intrinsic photon index range from 1.3 to 3.6 (Wagner 2008). If one smaller $F(E_\gamma > 300 \text{ GeV}) = 2.0 \times 10^{-12} \text{ cm}^{-2}\text{s}^{-1}$ is adopted, one larger $a_2 = 8.0$ is obtained. As $a_2 = 8.0$, photon indices of 3.3 ± 0.03 are inferred for $R_\gamma = 0.4$ pc, 3.6 ± 0.01 ($a_* = 0.5$) and 3.5 ± 0.003 ($a_* = 0.998$) for $R_\gamma = 0.25$ pc, and 7.3 ± 0.2 ($a_* = 0.5$) and 6.5 ± 0.2 ($a_* = 0.998$) for $R_\gamma = 0.1$ pc. Thus, larger photon indices of these pre-absorbed spectra are obtained for a fixed R_γ as larger a_2 is adopted. As $R_\gamma = r_{\text{BLR,in}}$, photon indices of these pre-absorbed gamma-ray spectra are always larger than the typical value $\Gamma_{\text{in}} = 2.3$ and the maximum $\Gamma_{\text{in}} = 3.6$ of those known intrinsic photon indices. Thus, it is unlikely for 3C 279 that R_γ be inside the BLR cavity, i.e. it is likely $R_\gamma > r_{\text{BLR,in}}$. If $F(E_\gamma > 300 \text{ GeV})$ adopted is closer to the upper limit of HESS observations, a_2 is not too large. Too large a_2 , such as $a_2 \simeq 10$ corresponding to $F(E_\gamma > 300 \text{ GeV}) \simeq 10^{-12} \text{ cm}^{-2}\text{s}^{-1}$, seems to be impossible for VHE gamma-ray spectra because these spectra with $a_2 \gtrsim 10$ are much steeper (softer) than the steepest (softest) spectrum measured for PG 1553+113 (Albert et al. 2007). When gamma-ray emitting region is already beyond the BLR, the EC mechanisms, where external photons originate from the BLR, are made inefficient to produce the observed gamma rays. For 3C 279, soft photon energy density around $r_{\text{BLR,out}}$ is lower by a factor of 6 to 7 than that around $r_{\text{BLR,in}}$ for the BLR diffuse radiation produced by the spherical shell of clouds (see Fig. 1 in Paper I). Thus it is unlikely $R_\gamma > r_{\text{BLR,out}}$, i.e. it is likely $R_\gamma \lesssim r_{\text{BLR,out}}$.

The external absorption softens the observed spectra relative to the emission ones in the interval from 10 GeV to 1 TeV. Whether the internal absorption softens or hardens the observed spectra relies on gamma-ray emitting radius R_γ and energy E_γ . Photon index variations of gamma-ray spectra relative to $a_2 = 6.4$ are calculated for the internal absorption, and the internal and external absorption (see Figure 7). As $R_\gamma = r_{\text{BLR,in}}$, the local photon indices of gamma-ray spectra decrease with E_γ from 10 to 110 GeV, and increase with E_γ from 110 GeV to 1 TeV (see Figure 7a). The local photon indices of gamma-ray spectra corrected for the internal absorption recover around 270 GeV ($\Delta\Gamma(\text{in}) = 0$). The internal absorption make gamma-ray spectra softer and softer from 10 to 110 GeV and from 270 down to 110 GeV, and make gamma-ray spectra harder and harder from 270 GeV to 1 TeV. After

corrected for the internal and external absorption, the local photon indices of gamma rays recover around 500 GeV ($\Delta\Gamma(\text{in} + \text{ext}) = 0$). The external absorption can not change the trend of the local photon indices of gamma-ray spectra corrected for the internal absorption. As $R_\gamma = (r_{\text{BLR,in}} + r_{\text{BLR,out}})/2$, the local photon indices of gamma-ray spectra corrected for the internal absorption behave as in the case of $R_\gamma = r_{\text{BLR,in}}$ (see Figure 7b). These local photon indices recover around 400 GeV ($\Delta\Gamma(\text{in}) = 0$). The internal absorption make gamma-ray spectra softer and softer from 10 to 110 GeV and from 400 down to 110 GeV, and make gamma-ray spectra harder and harder from 400 GeV to 1 TeV. After corrected for the internal and external absorption, the local photon indices of pre-absorbed gamma-ray spectra basically decrease with E_γ . The external absorption can not change the trend of the local photon indices of gamma-ray spectra corrected for the internal absorption below 100 GeV, but change that above 100 GeV. Gamma-ray spectra become softer and softer relative to pre-absorbed ones from 10 GeV to 1 TeV ($\Delta\Gamma(\text{in} + \text{ext}) < 0$). As $R_\gamma = r_{\text{BLR,out}}$, the local photon indices have similar trend to that in the case of $R_\gamma = (r_{\text{BLR,in}} + r_{\text{BLR,out}})/2$ (see Figure 7c). The internal absorption make gamma-ray spectra softer and softer from 10 to ~ 420 GeV and from 1 TeV down to ~ 420 GeV. After corrected for the internal and external absorption, the local photon indices monotonically decrease with E_γ , and gamma-ray spectra become softer and softer relative to pre-absorbed ones from 10 GeV to 1 TeV ($\Delta\Gamma(\text{in} + \text{ext}) < 0$). The external absorption change the trend of the local photon indices of gamma-ray spectra corrected for the internal absorption. The calculated results presented in Figure 7 basically are independent on the particular value of a_2 . For example, the trends of the local photon indices for $a_2 = 5.4$ are basically identical to those in the case of $a_2 = 6.4$. In summary, the internal absorption could make spectral shape more complex than only considering the external absorption, and could lead to the formation of arbitrary softening and hardening gamma-ray spectra (see Figs. 2–4 and 7). Thus, it should be necessary for the internal absorption to be considered in studying gamma rays of 10 GeV–1 TeV from FSRQs.

Assuming $\Gamma_{\text{jet}} = 15$ for 3C 279, most of gamma rays are contained within a radiation cone with a half open angle of $\Delta\varphi \sim 1/\Gamma_{\text{jet}} \sim 3.8^\circ$, because of the relativistic beaming effect. If the central IR–optical–UV photons coming directly from accretion disks travel through the radiation cone, the IR–optical–UV photons can have photon-photon pair creation processes with gamma rays within the radiation cone. The gamma-ray emitting region $R_\gamma \sim 0.1$ pc is assumed, and the radii of the UV radiation regions are $R_D \lesssim 30r_g \sim 0.0004$ pc (see Fig. 1), the angle between the jet direction and the travelling direction of UV photons at R_γ is $\sim \arcsin R_D/R_\gamma \lesssim 0.2^\circ$. Then the photons within the radiation cone have the collision angles of $\theta \lesssim 4.0^\circ$. For the UV photons at the frequency $\nu \simeq 10^{16.5}$ Hz with energies of $\varepsilon_2 \simeq 2.56 \times 10^{-4}$ and the gamma rays of $\varepsilon_1 \simeq 2.0 \times 10^6$ corresponding to energies around

1 TeV, the left of threshold condition (eq. [3] in Paper I) has an upper limit of $\lesssim 0.6$, which is less than unity, and thus the two kinds of photons cannot be absorbed by the photon-photon pair creation processes. Therefore, the central UV radiation has negligible contributions to the absorption for gamma rays relative to the diffuse radiation from the BLR. For optical photons, the radii of the optical radiation regions are $R_D < 200r_g \sim 0.003$ pc, the angle between the jet direction and the travelling direction of optical photons at R_γ is $\sim \arcsin R_D/R_\gamma \lesssim 1.7^\circ$. Then the photons within the radiation cone have the collision angles of $\theta \lesssim 5.5^\circ$. For the optical photons at the frequency $\nu \simeq 10^{15}$ Hz with energies of $\varepsilon_2 \simeq 8.1 \times 10^{-6}$ and the gamma rays of $\varepsilon_1 \simeq 2.0 \times 10^6$, the left of threshold condition has an upper limit of $\lesssim 0.04$, which is less than unity, and thus the two kinds of photons cannot be absorbed by the photon-photon pair creation processes. Therefore, the central optical radiation has negligible contributions to the absorption for gamma rays relative to the diffuse radiation from the BLR. For IR photons, the central radiation also has negligible contributions to the absorption for gamma rays. Thus, the central IR–optical–UV radiation has negligible contributions to the absorption for gamma rays relative to the diffuse radiation from the BLR.

Absorption for gamma rays by photon-photon annihilation and where the energies carried by the annihilated gamma rays reradiate are important to gamma-ray research. The intense creation of pairs would produce a strong radiation at low energy X-rays or at GeV energy (Protheroe & Stanev 1993; Saugé & Henri 2004; Zdziarski & Coppi 1991). The electron-positron pair cascade could cause the soft X-ray excesses (Zdziarski & Coppi 1991). The produced electron-positron pairs could make a difference around 1 GeV, where the pileup of photons below the absorption threshold results in a significant flattening in the observed spectrum relative to the emission spectrum (Protheroe & Stanev 1993). In § 6, we studied the pair spectrum due to photon-photon absorption, and the synchrotron and EC spectra emitted by the equilibrium pair distribution of steady state. The synchrotron radiation peaks around keV X-rays, and the EC radiation peaks around GeV gamma rays (see Fig. 6b). Thus, pairs due to annihilation absorption for gamma rays by the diffuse radiation fields of the BLR are likely to make a difference around 1 GeV for 3C 279.

In this paper, in order to limit the gamma-ray emitting radius R_γ , we used a BLR model to study the photon-photon absorption by the diffuse radiation of the BLR in 3C 279 for gamma rays of 10 GeV to 1 TeV in the observed spectrum. We calculated the internal absorption of gamma rays from 10 GeV to 1 TeV for $R_\gamma = r_{\text{BLR,in}}$, $r_{\text{BLR,out}}$, and $(r_{\text{BLR,in}} + r_{\text{BLR,out}})/2$ (see Figs. 2a, 3a, and 4a). For a fixed R_γ , dependence of photon-photon absorption optical depth $\tau_{\gamma\gamma}$ on energies of gamma rays E_γ relies on R_γ . Dependence of $\tau_{\gamma\gamma}$ on R_γ was also studied for a fixed E_γ (see Fig. 5). For a fixed E_γ , $\tau_{\gamma\gamma}$ decreases with increasing R_γ . The external absorption on the IR–optical–UV EBL was also estimated for

gamma rays of 10 GeV–1 TeV, and it monotonically increases as E_γ increases. Comparing the internal absorption with the external one shows that R_γ determines the relative contributions of the internal and external absorption to the total photon-photon annihilation absorption of 10 GeV–1 TeV gamma rays (see Figs. 2a, 3a, and 4a). Based on MAGIC and HESS observations, a power-law spectrum as in equation (1) was adopted for the photon intensity of VHE gamma rays. The pre-absorbed gamma-ray spectra are inferred by this power-law corrected for the internal and external absorption. The internal absorption could make spectral shape of gamma rays more complex than that only corrected for the external absorption, and could lead to the formation of arbitrary softening and hardening gamma-ray spectra (see Figs. 2a, 3a, 4a, and 7). Thus, it should be necessary for the internal absorption to be considered in studying 10 GeV–1 TeV gamma rays from FSRQs. R_γ significantly influences the variations of spectral shape due to the internal absorption. Calculations imply that the energies of annihilated gamma rays due to the internal absorption are mainly reradiated around GeV regime (see Fig. 6b). Considering the possible variations of photon index a_2 , the photon indices of the pre-absorbed VHE gamma-ray spectra were compared with those known intrinsic photon indices. As $R_\gamma = r_{\text{BLR,in}}$ and $a_2 \gtrsim 6.4$, the photon indices of the pre-absorbed gamma-ray spectra are always larger than the typical value $\Gamma_{\text{in}} = 2.3$ and the maximum $\Gamma_{\text{in}} = 3.6$ of those known intrinsic photon indices, and $\tau_{\gamma\gamma}$ is larger than unity. Thus, it is likely $R_\gamma > r_{\text{BLR,in}}$ for 3C 279. As $R_\gamma = r_{\text{BLR,out}}$ and $6.4 \lesssim a_2 \lesssim 8.3$, photon indices of pre-absorbed gamma-ray spectra are not larger than $\Gamma_{\text{in}} = 3.6$. For a fixed a_2 , photon indices of pre-absorbed gamma-ray spectra decrease as R_γ increases. Too large a_2 seems to be impossible for VHE gamma-ray spectra. In addition, the EC processes may be inefficient to produce the observed gamma rays as gamma-ray emitting region is already beyond the BLR. Thus, it is likely $R_\gamma \lesssim r_{\text{BLR,out}}$ for 3C 279. Our results suggest that R_γ for powerful blazars might be neither inside the BLR cavity nor outside the BLR, but be within the BLR shell. This is neither consistent with suggestions of Ghisellini & Madau (1996) and Georganopoulos et al. (2001) nor consistent with suggestions of Lindfors et al. (2005) and Sokolov & Marscher (2005).

Our results are model dependent, especially dependent on the assumed power-law spectrum for the VHE gamma rays. If Teshima et al. published the spectral indices of gamma-ray spectra measured by MAGIC (Teshima et al. 2007), the power-law spectrum assumed in this paper could be tested. Tavecchio & Ghisellini (2008) used the photoionization code CLOUDY, described by Ferland et al. (1998), to calculate the detailed spectra from the BLRs for powerful blazars, and then used these spectra to calculate the EC spectra. Approximate spectra of the BLRs are used in this paper and Paper I, and another approximate spectra are used by Reimer (2007). Difference between the detailed and approximate spectra should exist. It should be useful in the future researches to study the effects of this

difference on the results of previous researches using approximate spectra (e.g., Liu & Bai 2006; Reimer 2007). Observations of *GLAST*, MAGIC, HESS, and VERITAS in the near future could give more observational constraints on the gamma-ray emitting regions and the BLRs for the powerful blazars. Publications of intrinsic photon indices predicted by theoretical researches and photon indices measured by observations in the VHE regime could give stronger constraints on R_γ .

We are grateful to the anonymous referee for his/her constructive comments and suggestions leading to significant improvement of this paper. H. T. L. thanks for financial support by National Natural Science Foundation of China (NSFC, Grant 10573030) and (Grant 10778726). L. M. is supported by NSFC (Grant 10778702). J. M. B. thanks support of the Bai Ren Ji Hua project of the CAS, China.

A. Appendix

If the central black holes are Kerr ones, the local effective temperature of the standard disk is given in the Kerr metric as (Krolik 1999)

$$T_{\text{eff}}(X_d) = \left[\frac{3GM_{\text{BH}}\dot{M}}{8\pi\sigma_{\text{SB}}r_g^3X_d^3}R_{\text{R}}(X_d) \right]^{1/4}, \quad (\text{A1})$$

where σ_{SB} is the Stefan-Boltzmann constant, M_{BH} is the black hole mass, \dot{M} is the mass accretion rate of the central black hole, and the function $R_{\text{R}}(X_d)$ is

$$R_{\text{R}}(X_d) = \frac{C(X_d)}{B(X_d)}, \quad (\text{A2})$$

where the functions $B(X_d)$ and $C(X_d)$ are, respectively, (Krolik 1999)

$$B(X_d) = 1 - \frac{3}{X_d} + \frac{2a_*}{X_d^{3/2}}, \quad (\text{A3})$$

$$\begin{aligned} C(X_d) = & 1 - \frac{y_{\text{ms}}}{y} - \frac{3a_*}{2y} \ln \left(\frac{y}{y_{\text{ms}}} \right) \\ & - \frac{3(y_1 - a_*)^2}{yy_1(y_1 - y_2)(y_1 - y_3)} \ln \left(\frac{y - y_1}{y_{\text{ms}} - y_1} \right) \\ & - \frac{3(y_2 - a_*)^2}{yy_2(y_2 - y_1)(y_2 - y_3)} \ln \left(\frac{y - y_2}{y_{\text{ms}} - y_2} \right) \\ & - \frac{3(y_3 - a_*)^2}{yy_3(y_3 - y_1)(y_3 - y_2)} \ln \left(\frac{y - y_3}{y_{\text{ms}} - y_3} \right), \end{aligned} \quad (\text{A4})$$

where $y = (X_d)^{1/2}$, $a_* = cJ/GM_{\text{BH}}^2$ is the dimensionless spin parameter of the central black hole with the spin angular momentum J , $y_{\text{ms}} = (X_{\text{ms}})^{1/2}$ is the value of y at the marginally stable orbit, and $y_{1,2,3}$ are the three roots of $y^3 - 3y + 2a_* = 0$ (see e.g., Reynolds & Nowak 2003).

Assuming prograde orbits, the radii of the marginally stable orbits in the equatorial plane of a Kerr black hole are (Bardeen et al. 1972)

$$X_{\text{ms}} = 3 + Z_2 - [(3 - Z_1)(3 + Z_1 + 2Z_2)]^{1/2}, \quad (\text{A5})$$

where

$$Z_1 = 1 + (1 - a_*^2)^{1/3} \left[(1 + a_*)^{1/3} + (1 - a_*)^{1/3} \right], \quad (\text{A6})$$

and

$$Z_2 = (3a_*^2 + Z_1^2)^{1/2}. \quad (\text{A7})$$

The marginally stable orbits in the equatorial plane correspond to the maximum efficiency of energy release as a result of accretion, assuming prograde orbits (Kembhavi & Narlika 1999)

$$\eta_{\text{max}} = 1 - \frac{X_{\text{ms}} - 2 + a_* X_{\text{ms}}^{-1/2}}{\sqrt{X_{\text{ms}} (X_{\text{ms}} - 3 + 2a_* X_{\text{ms}}^{-1/2})}}. \quad (\text{A8})$$

REFERENCES

- Aharonian, F. A., Atoyan, A. M., & Nagapetyan, A. M. 1983, *Astrophysics*, 19, 187
- Aharonian, F. et al., 2008, *A&A*, 478, 387
- Albert, J. et al., 2007, *ApJ*, 654, L119
- Aschenbach, B., Grosso, N., Porquet, D., & Predehl, P. 2004, *A&A*, 417, 71
- Baixeras, C. et al., 2004, *NIMPA*, 518, 188
- Bardeen, J. M., Press, W. H., & Teukolsky, S. A. 1972, *ApJ*, 178, 347
- Blandford, R. D., & Levison, A. 1995, *ApJ*, 441, 79
- Blandford, R. D., & Rees, M. J. 1978, in *Pittsburgh Conf. on BL Lac Objects*, ed. A. M. Wolfe (Pittsburgh: Univ. Pittsburgh Press), 328
- Blumenthal, G., & Gould, R. 1970, *Rev. Mod. Phys.*, 42, 237
- Böttcher, M., & Schlickeiser, R. 1997, *A&A*, 325, 866

- Böttcher, M. 1999, in AIP Conf. Proc. 515, GeV-TeV Gamma Ray Astrophysics Workshop, ed. B. L. Dingus, M. H. Salamon, & D. B. Kieda (New York: AIP), 31
- Böttcher, M., et al. 2007, ApJ, 670, 968
- Brenneman, L. W., & Reynolds, C. S. 2006, ApJ, 652, 1028
- Cao, X. W., & Jiang, D. R. 1999, MNRAS, 307, 802
- Catanese, M., et al. 1997, ApJ, 487, L143
- Chen, A., Reyes, L. C., & Ritz, S. 2004, ApJ, 608, 686
- Crusius, A., & Schlickeiser, R. 1986, A&A, 164, L16
- D’Elia, V., Padovani, P., & Landt H. 2003, MNRAS, 339, 1081
- Donea, A. C., & Protheroe, R. J. 2003, Astropart. Phys., 18, 377
- Dwek, E., & Krennrich, F. 2005, ApJ, 618, 657
- Ebisawa, K., Mitsuda, K., & Hanawa, T. 1991, ApJ, 367, 213
- Ferland, G. J., Korista, K. T., Verner, D. A., Ferguson, J. W., Kingdon, J. B., & Verner, E. M. 1998, PASP, 110, 761
- Fichtel, C. E., et al. 1994, ApJS, 94, 551
- Funk, S. et al., 2004, Astropart. Phys., 22, 285
- Gammie, C. F., Shapiro, S. L., & McKinney, J. C. 2004, ApJ, 602, 312
- Gehrels, N., & Michelson, P. 1999, Astropart. Phys., 11, 277
- Georganopoulos, M., Kirk, J. G., & Mastichiadis, A. 2001, in ASP Conf. Series 227, Blazar Demographics and Physics, Ed. P. Padovani and C. M. Urry (San Francisco: Astronomical Society of the Pacific), 116
- Ghisellini, G., Guilbert, P., & Svensson, R. 1988, ApJ, 334, L5
- Ghisellini, G., & Madau, P. 1996, MNRAS, 280, 67
- Ghisellini, G., Celotti, A., Fossati, G., Maraschi, L., & Comastri, A. 1998, MNRAS, 301, 451
- Hanawa, T. 1989, ApJ, 341, 948
- Hartman, R. C., et al. 1999, ApJS, 123, 79
- Hartman, R. C., et al. 2001a, ApJ, 558, 583;
- Hartman, R. C., et al. 2001b, ApJ, 553, 683
- Hinton, J. A. 2004, New Astron. Rev., 48, 331

- Hofmann, W. 2003, Proc. 28th ICRC (Tsukuba), 2811
- Holder, J., et al. 2006, *Astroparticle Physics*, 25, 391
- Jones, F. C. 1968, *Phys. Rev.*, 167, 1159
- Kartaltepe, J., & Balonek, T. J. 2007, *AJ*, 133, 2866
- Kemhavi, A. K., & Narlika, J. V 1999, *Quasars and Active Galactic Nuclei: An introduction* (Cambridge: Cambridge Univ. Press), p107
- Krolik, J. H. 1999, *Active Galactic Nuclei: From the Central Black Hole to the Galactic Environment* (Princeton: Princeton Univ. Press), p151–154
- Krolik, J. H., Hawley, J. F., & Hirose, S. 2005, *ApJ*, 622, 1008
- Li, L. X., Zimmerman, E. R., Narayan, R., & McClintock, J. E. 2005, *ApJS*, 157, 335
- Lin, Y. C., et al. 1997, *ApJ*, 476, L11
- Lindfors, E. J., Valtaoja, E., & Turler, M. 2005, *A&A*, 440, 845
- Liu, H. T., & Bai, J. M. 2006, *ApJ*, 653, 1089 (Paper I)
- Liu, H. T., Bai, J. M., Zhao X. H., & Ma, L. 2008, *ApJ*, 677, 884
- Maiolino, R., Salvati, M., Marconi, A., & Antonucci, R. R. J. 2001, *A&A*, 375, 25
- Mukherjee, R., et al. 1997, *ApJ*, 490, 116
- Nolan, P. L., Tompkins, W. F., Grenier, I. A., & Michelson, P. F 2003, *ApJ*, 597, 615
- Oh, S. P. 2001, *ApJ*, 553, 25
- Pereyra, N. A., Berk, D. E. V., Turnshek, D. A., & Hillier, D. J. 2006, *ApJ*, 642, 87
- Protheroe, R. J., & Stanev, T. 1993, *MNRAS*, 264, 191
- Punch, M., et al. 1992, *Nature*, 358, 477
- Quinn, J., et al. 1996, *ApJ*, 456, L83
- Renault, C., Barrau, A., Lagache, G., & Puget, J. L. 2001, *A&A*, 371, 771
- Reimer, A. 2007, *ApJ*, 665, 1023
- Reynolds, C. S., & Nowak, M. A. 2003, *Physics Reports*, 377, 389
- Saugé, L., & Henri, G. 2004, *ApJ*, 616, 136
- Schroedter, M. 2005, *ApJ*, 628, 617
- Shakura, N. I., & Sunyaev, R. A. 1973, *A&A*, 24, 337
- Sokolov, A. & Marscher, A. P. 2005, *ApJ*, 629, 52
- Stecker, F. W., de Jager, O. C., & Salamon, M. H. 1992, *ApJL*, 390, 49

- Stecker, F. W., & de Jager, O. C. 1998, *A&A*, 334, L85
- Stecker, F. W., Malkan, M. A., & Scully, S. T. 2006, *ApJ*, 648, 774
- Stecker, F. W., Malkan, M. A., & Scully, S. T. 2007, *ApJ*, 658, 1392
- Tavecchio, F., & Ghisellini, G. 2008, *MNRAS*, 386, 945
- Teshima, M., et al. (MAGIC collaboration), 2007, in Proc. 30th International Cosmic Ray Conference. Preprint (arXiv:0709.1475)
- Thompson, D. J., et al. 1995, *ApJS*, 101, 259
- Thompson, D. J., et al. 1996, *ApJS*, 107, 227
- Thorne, K. S. 1974, *ApJ*, 191, 507
- Venters, T. M., & Pavlidou, V. 2007, *ApJ*, 666, 128
- Villata, M., et al. 1997, *A&AS*, 121, 119
- von Montigny, C., et al. 1995, *ApJ*, 440, 525
- Wagner, R. M. 2008, *MNRAS*, 385, 119
- Wehrle, A. E., et al. 1998, *ApJ*, 497, 178
- Woo, J. H., & Urry, C. M. 2002, *ApJ*, 579, 530
- Zdziarski, A. A., & Coppi, P. S. 1991, *ApJ*, 376, 480
- Zimmerman, E. R., Narayan, R., McClintock, J. E., & Miller, J. M. 2005, *ApJ*, 618, 832

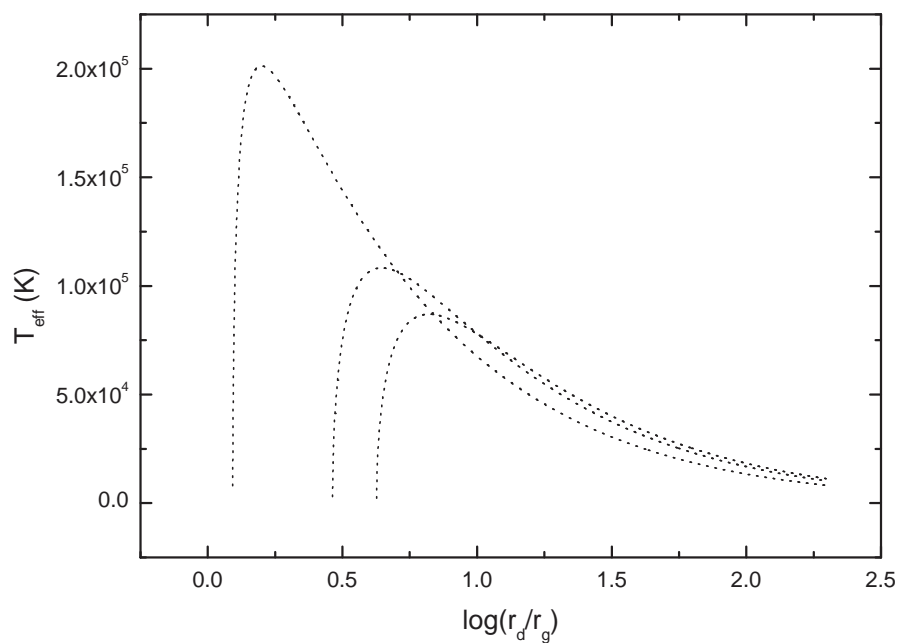


Fig. 1.— Radial profiles of T_{eff} shown in the basis of the standard accretion disk under the Kerr potential for 3C 279. The curves are calculated by adopting $f_{\text{cov}} = 0.03$, $L_{\text{BLR}} = 10^{44.41}$ ergs s $^{-1}$, and $M_{\text{BH}} = 10^{8.4} M_{\odot}$. From the top down, the curves correspond to $a_* = 0.998$, $a_* = 0.8$, and $a_* = 0.5$, respectively.

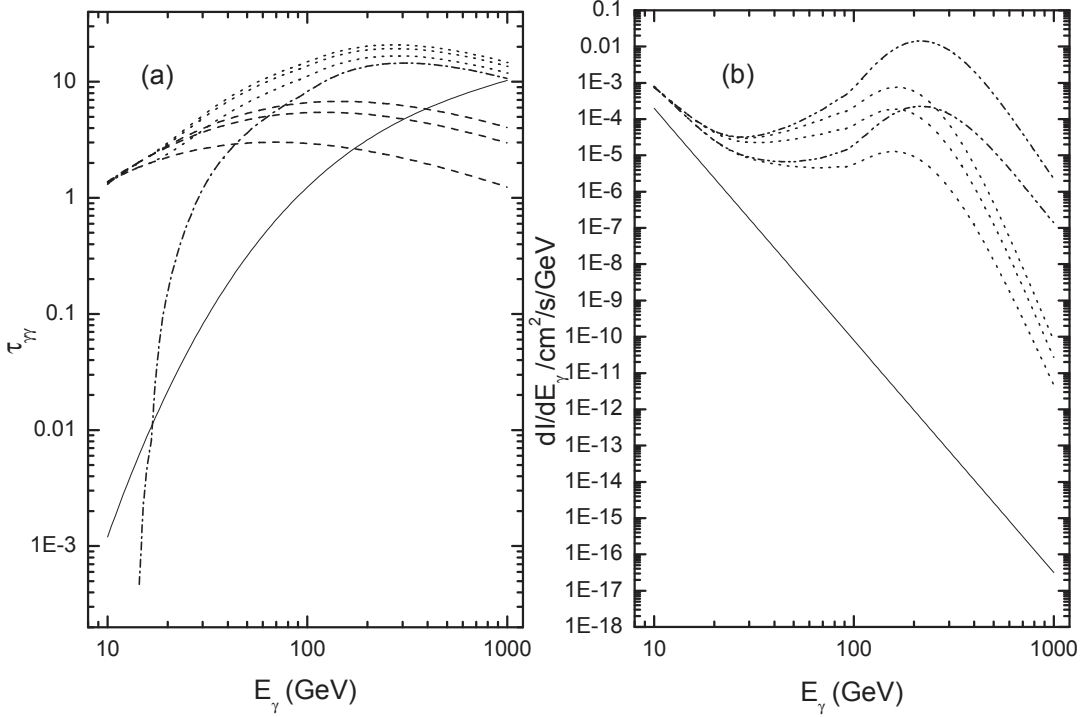


Fig. 2.— Plot (a) is photon-photon absorption optical depth for 3C 279. Dashed lines are absorption by multi-temperature blackbody, dash-dotted line is absorption by broad emission lines, and dotted lines are the total absorption by the two radiation fields. In calculations of $\tau_{\gamma\gamma}$, we assumed $R_\gamma = r_{\text{BLR},\text{in}}$, $\tau_{\text{BLR}}/f_{\text{cov}} = 1$, and $f_{\text{cov}} = 0.03$, and adopted $r_{\text{BLR},\text{in}} = 0.1$ pc, $r_{\text{BLR},\text{out}} = 0.4$ pc, $L_{\text{BLR}} = 10^{44.41}$ ergs s^{-1} , and $M_{\text{BH}} = 10^{8.4} M_\odot$. Plot (b) is gamma-ray spectrum of 3C 279: the spectrum expressed by equation (1) (solid line), and the corrected spectra for photon-photon absorption by the diffuse radiation fields of BLR (dotted lines). From the top down, dotted and dashed curves in plot (a) are calculated by assuming $a_* = 0.5$, $a_* = 0.8$, and $a_* = 0.998$, respectively. From the top down, dotted curves in plot (b) are calculated by assuming $a_* = 0.998$, $a_* = 0.8$, and $a_* = 0.5$, respectively. Solid line in plot (a) is the external absorption due to the EBL, estimated by equation (4). Dash-dot-dotted lines in plot (b) correspond to the dotted lines in plot (a), in the case of $a_* = 0.5$ and $a_* = 0.998$, but corrected for the EBL absorption.

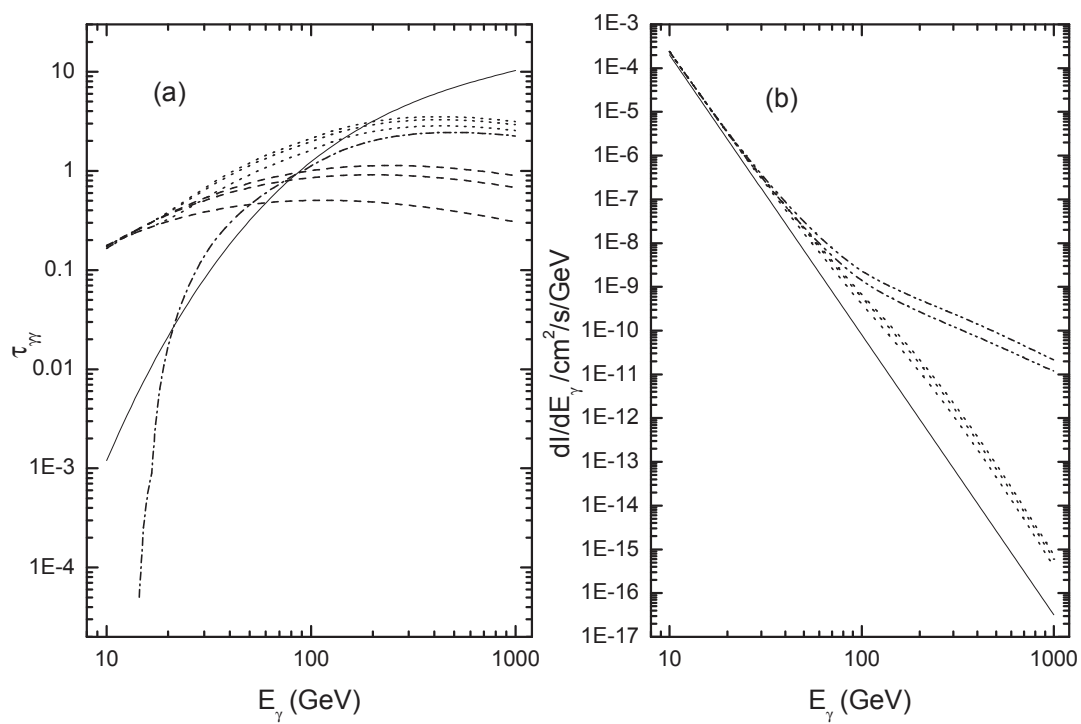


Fig. 3.— The patterns of lines are the same as ones in Figure 2 with the same parameters except for $R_\gamma = (r_{\text{BLR,in}} + r_{\text{BLR,out}})/2 = 0.25$ pc.

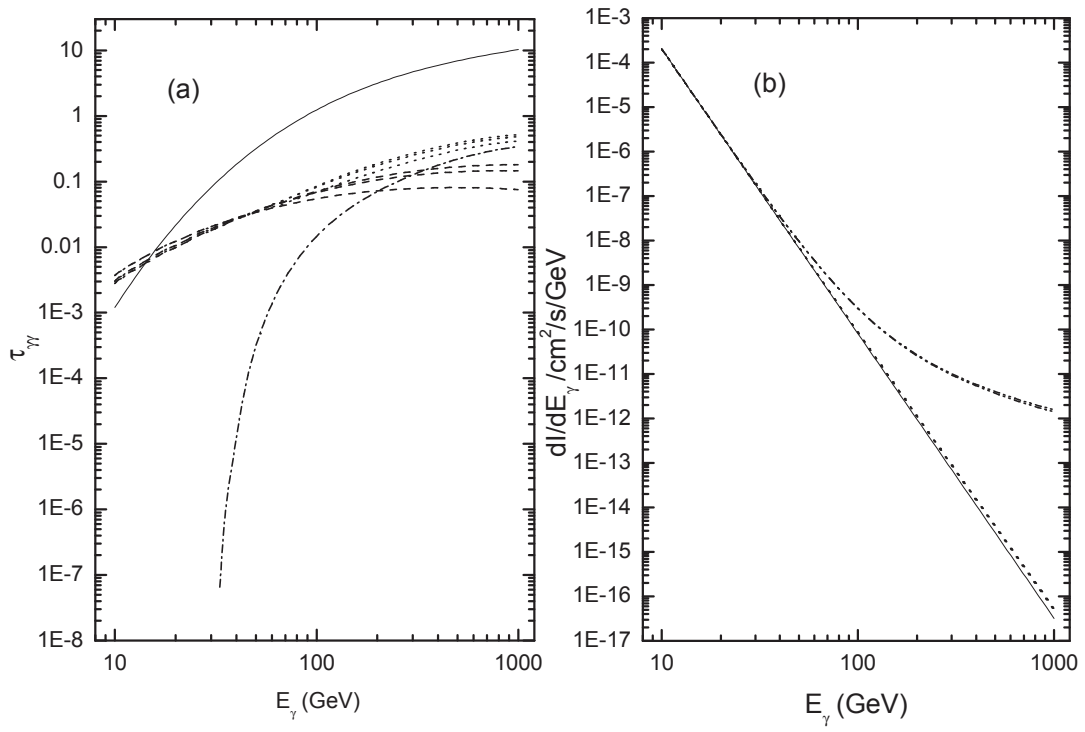


Fig. 4.— The patterns of lines are the same as ones in Figure 2 with the same parameters except for $R_{\gamma} = r_{\text{BLR,out}}$.

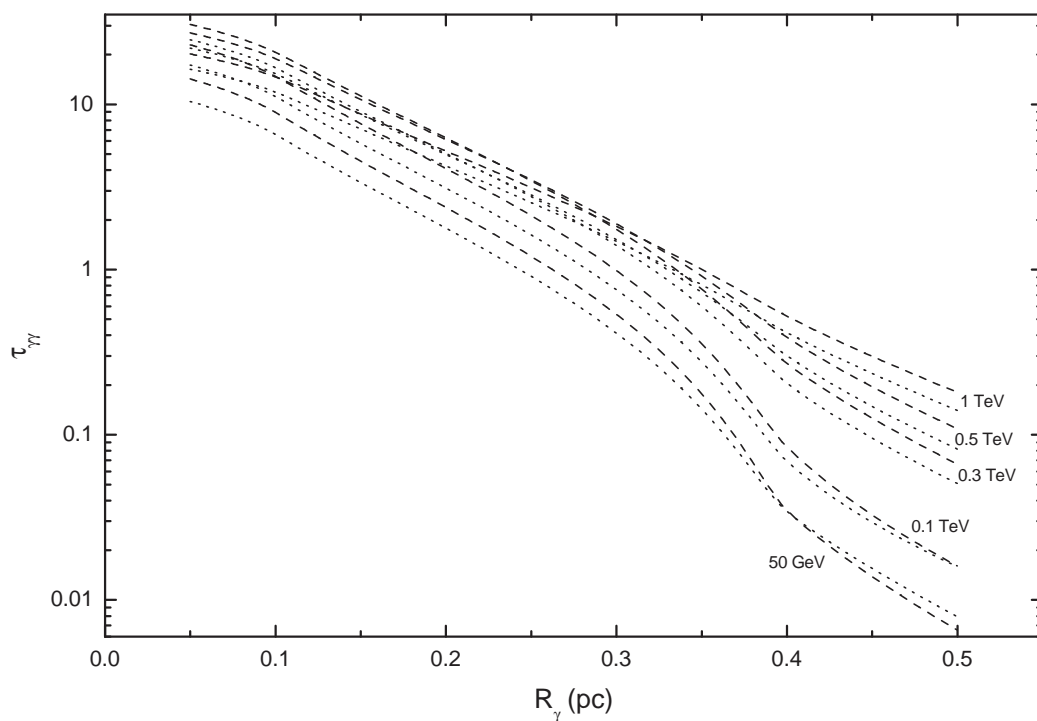


Fig. 5.— Dependence of $\tau_{\gamma\gamma}$ on R_γ . Dotted lines are the absorption optical depth in the case of $a_* = 0.998$, and dashed lines $a_* = 0.5$.

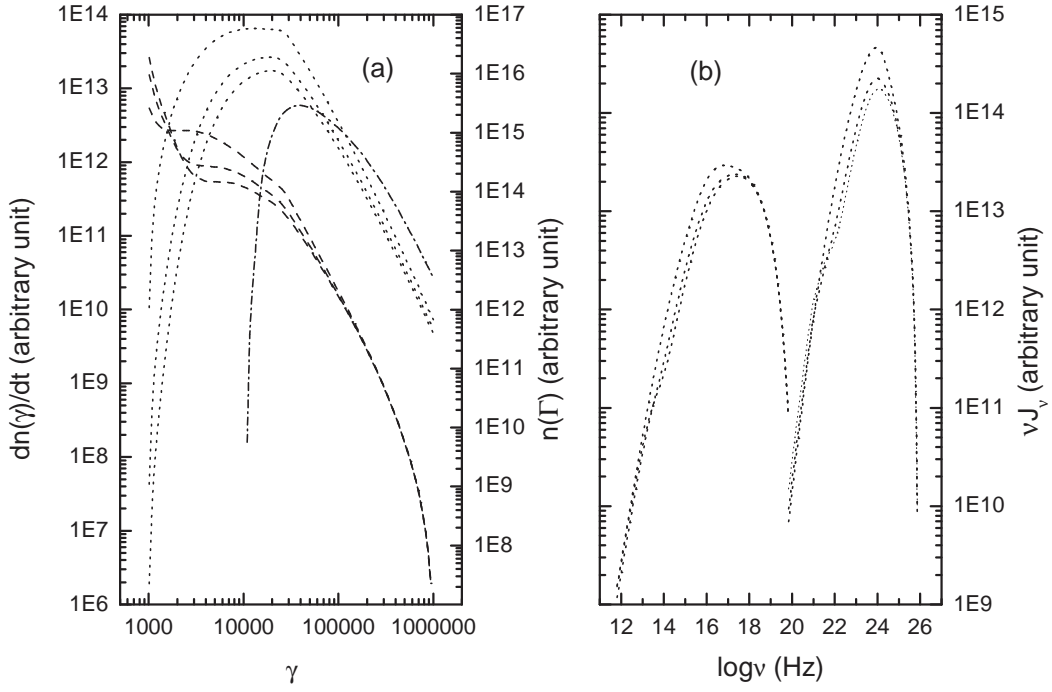


Fig. 6.— Pair production spectrum from photon-photon annihilation. Plots show (a) the differential pair production rate produced by gamma rays (assumed as $\propto E_\gamma^{-2.3}$) and multi-temperature blackbody (dotted curves), the one produced by gamma rays and broad emission lines (dash-dotted curve), and the total equilibrium pair distribution for the two pair production rate (dashed curves); (b) the synchrotron and EC spectra emitted by the equilibrium pair distribution. The curves are calculated by adopting $f_{\text{cov}} = 0.03$, $L_{\text{BLR}} = 10^{44.41}$ ergs s $^{-1}$, and $M_{\text{BH}} = 10^{8.4} M_\odot$. From the top down, dotted and dashed curves correspond to $a_* = 0.998$, $a_* = 0.8$, and $a_* = 0.5$, respectively.

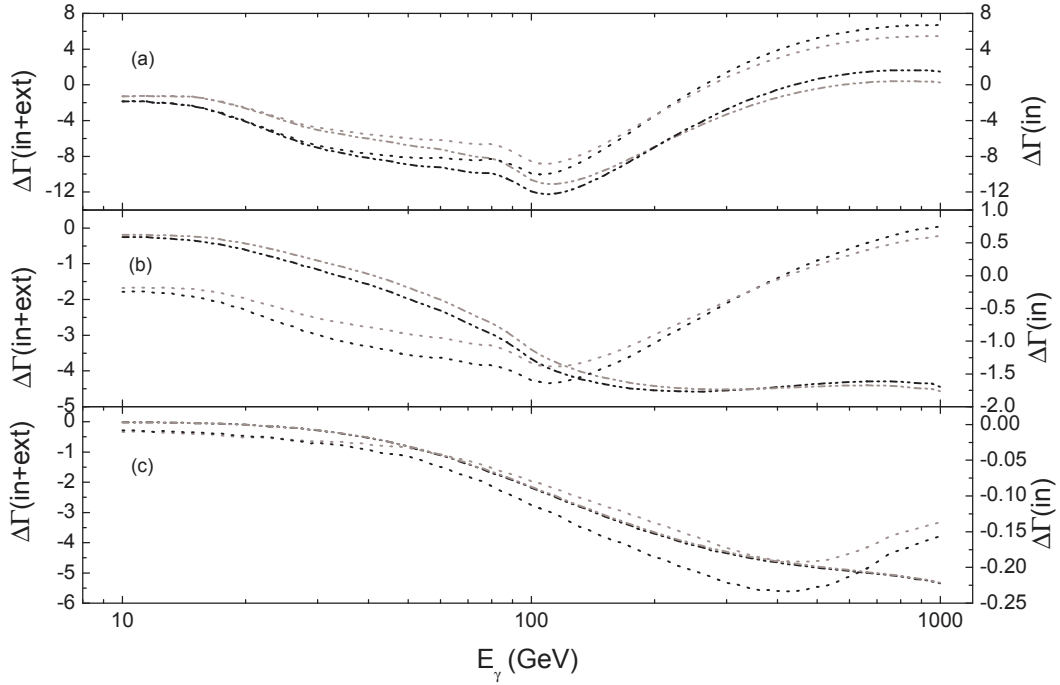


Fig. 7.— Photon index variations of gamma-ray spectra presented in Figures 2*b*, 3*b*, and 4*b*. (a) $R_\gamma = r_{\text{BLR,in}}$. (b) $R_\gamma = (r_{\text{BLR,in}} + r_{\text{BLR,out}})/2$. (c) $R_\gamma = r_{\text{BLR,out}}$. Gray curves are calculated by adopting $a_* = 0.998$, and black curves $a_* = 0.5$. Dotted curves present gamma-ray spectra corrected for the internal absorption, and dash-dot-dotted curves these corrected for the internal and external absorption.